Oxygen substitution effects in Li$_{10}$GeP$_2$S$_{12}$ solid electrolyte

CrossMark

Yulong Sun [a], Kota Suzuki [a, b], Kosuke Hara [a], Satoshi Hori [a], Taka-aki Yano [a, b], Masahiko Hara [a, b], Masaaki Hirayama [a, b], Ryoji Kanno [a, b, *]

[a] Department of Electronic Chemistry, Interdisciplinary Graduate School of Science and Engineering, Tokyo Institute of Technology, 4259 Nagatsuta, Midori-ku, Yokohama 226-8502, Japan
[b] Department of Chemical Science and Engineering, School of Materials and Chemical Technology, Tokyo Institute of Technology, 4259 Nagatsuta, Midori-ku, Yokohama 226-8502, Japan

HIGHLIGHTS

- Partial sulfur substitution by oxygen was demonstrated for Li$_{10}$GeP$_2$S$_{12}$.
- The solid solution range was found to be $0 \leq x < 0.9$ in Li$_{10}$GeP$_2$S$_{12-x}$O$_x$.
- Li$_{10}$GeP$_2$S$_{12-x}$O$_x$ showed high electrochemical stability at low potential.
- Preferred substitution to form the P(S/O)$_4$ unit in the structure was confirmed.
- A high ionic conductivity of 10^{-2} S cm^{-1} was maintained after substitution.

ARTICLE INFO

ABSTRACT

For the lithium super-ionic conductor Li$_{10}$GeP$_2$S$_{12}$, the partial substitution of sulfur by oxygen is achieved via a solid-state reaction. The solid-solution range of oxygen is found to be $0 \leq x < 0.9$ in Li$_{10}$GeP$_2$S$_{12-x}$O$_x$. Structure refinements using synchrotron X-ray diffraction data confirm the preference for oxygen substitution in the PS$_4$ tetrahedra. The local structural change in the P(S/O)$_4$ tetrahedra upon substitution is also indicated by Raman spectroscopy. Ionic conduction properties are maintained even after the oxygen substitution in Li$_{10}$GeP$_2$S$_{12}$; the ionic conductivity of Li$_{10}$GeP$_2$S$_{12-x}$O$_x$ ($0.3 \leq x \leq 0.6$) ranges from 1.03×10^{-2} to 8.43×10^{-3} S cm^{-1} at 298 K. No redox current is observed by cyclic voltammetry from nearly 0 to 10 V versus Li/Li$^+$ except for that due to the lithium deposition/dissolution reactions. All-solid-state batteries using Li$_{10}$GeP$_2$S$_{12-x}$O$_x$ ($x = 0.3$ and 0.6) as solid electrolytes with Li metal anodes show discharge capacities exceeding 100 mAh g^{-1} and better cycling performance compared to batteries using the original Li$_{10}$GeP$_2$S$_{12}$. The partial substitution of oxygen for sulfur in Li$_{10}$GeP$_2$S$_{12}$ affords a novel solid electrolyte, Li$_{10}$GeP$_2$S$_{12-x}$O$_x$, with high conductive properties and electrochemical stability.

1. Introduction

Lithium-ion conducting solids, as key materials for solid electrolytes in all-solid-state lithium batteries, have great potential for improving the safety, reliability, energy density, and power density of lithium battery systems [1]. Among the reported solid electrolytes, sulfide-based materials are attractive due to their superior properties compared to their oxide counterparts. One of the most remarkable advantages of sulfides is their notable ionic conductivity, which can be as high as 10^{-3}–10^{-2} S cm^{-1} [2–5]. Moreover, the grain-boundary resistance of sulfides is easily reduced, which is suitable for application in bulk-type all-solid-state batteries [6–8]. Furthermore, a wide range of solid solutions, and thus, material properties, are accessible through the substitution of elements in the system [2,9]. Therefore, sulfide-based solid electrolytes have been intensively studied as promising components of all-solid-state lithium batteries. Li$_{10}$GeP$_2$S$_{12}$ (LGPS), belonging to the sulfide family, exhibits an extremely high ionic conductivity of 1.2×10^{-2} S cm^{-1}, a value comparable to those of the liquid electrolytes used in commercial lithium-ion batteries [10]. However, LGPS is not stable against Li metal, which provides the highest

battery voltage, because it decomposes at the low voltage triggered by the reduction of Ge [11]. Therefore, it would be significant to develop new solid electrolytes having both high ionic conductivity and high electrochemical stability.

In the design of new ionic conductors, one approach is to modify existing materials with suitable frameworks for ionic conduction. The discovery of LGPS afforded a structural template for exploring new solid electrolytes. After this discovery, many kinds of new solid electrolytes belonging to the LGPS family, such as $Li_{10}SiP_2S_{12}$, $Li_{10}SnP_2S_{12}$, and $Li_{11}AlP_2S_{12}$, were predicted by first principles calculations [12]. The subsequent synthesis of several of these materials [13–17] shows that a wide range of solid-solutions in the LGPS family would be available through the appropriate selection of elements (anions and cations). Given that the chemical bonds between Ge/P−O are stronger than those of Ge/P−S, oxygen substitution would be expected to enhance thermodynamic stability. Density-of-states (DOS) results from first principles calculations also predict that O-substituted LGPS-type LMPO materials would exhibit greater intrinsic redox stability than LMPS compounds [12]. For example, oxysulfide systems are reported to achieve higher electrochemical stabilities [18–20]: the LGPS-type Ge-free Li−P−S−O system with enhanced stability in the low voltage region was proposed, however, its conductive properties were decreased to 10^{-4}–10^{-5} S cm^{-1} [20]. Therefore, based on the concept of developing LGPS-type ionic conductors, oxygen introduction into the LGPS crystal structure would be expected to improve electrochemical stability while maintaining relatively high ionic conductivity [21].

In this study, the substitution of oxygen for sulfur in the LGPS structure was examined; new solid electrolytes with the compositions $Li_{10}GeP_2S_{12-x}O_x$ ($0 < x \leq 1.5$) were synthesized, and their crystal structures, ionic conductivities and electrochemical stabilities were investigated. The battery performance of the all-solid-state cells using the newly developed $Li_{10}GeP_2S_{12-x}O_x$ solid electrolytes was also examined.

2. Experimental

The oxygen-substituted LGPS materials were fabricated based on the composition $Li_{10}GeP_2S_{12-x}O_x$. The starting materials, Li_2S (Nihon Kagaku Kogyo, >99.9% purity), GeS_2 (Mitsuwa Chemical, 99.9% purity), Li_2O (Kojundo Chemical Laboratory Co., Ltd., >99.9% purity), and P_2S_5 (Aldrich, > 99.9% purity), were weighed in stoichiometric ratios in an Ar-filled glove box, and then mixed mechanically in a ZrO_2 pot with ZrO_2 balls ($\varphi = 10$ mm). The mixing process was conducted using a planetary ball milling apparatus at 380 rpm for 20 h. The product mixture was pelletized under 120 MPa pressure, sealed in a quartz tube at ~10 Pa, and heated at 823 K for 24 h. Then, the samples were slowly cooled to room temperature.

X-ray diffraction patterns of the synthesized powders were collected using an X-ray diffractometer (Rigaku Smartlab) with Cu Kα radiation. The diffraction data were collected at a 0.01° step width over a 2θ range from 10 to 50°. Synchrotron X-ray diffraction measurements were performed using the BL02B2 beamline at SPring-8, with an X-ray wavelength of 0.5 Å. The specimens were sealed under Ar atmosphere in Lindemann glass capillaries (~0.3 mm inner diameter), and a Debye-Scherrer diffraction camera was employed for the measurements. Diffraction data were collected in 0.01° steps from 3 to 70° at room temperature. Refinements for the structural parameters were conducted using the RIETAN-FP program [22]. Raman spectral measurements were performed to observe the local structure in the $Li_{3.35}Ge_{0.35}P_{0.65}S_{4-x}O_x$ using a confocal Raman microscope (Raman 11, Nanophoton Corp.) with an excitation wavelength of 532 nm.

Ionic conductivity was measured by the alternating current (AC) impedance method with an applied voltage of 20 mV in the frequency range from 100 Hz to 15 MHz using a frequency response analyzer (National Instruments, NF) in an Ar-gas-cycled atmosphere over the temperature range 298−398 K. For the measurements, pellets of the solid electrolytes (diameter ≈ 10 mm; thickness 1−2 mm) were prepared by the cold-press method under 168 MPa and then sintered at 823 K for 12 h. Both surfaces of the sintered pellets were coated with Au powder to form blocking electrodes. The electrochemical stability was evaluated by cyclic voltammetry. The measurements were conducted in a Li/solid electrolyte (SE)/Au cell at a scan rate of 1 mV s^{-1} between −0.5 to 10 V using a Solartron 1287 electrochemical interface.

The fabrication of two-electrode all-solid-state batteries using the prepared solid electrolytes was conducted under Ar atmosphere. Composite electrodes incorporating $LiCoO_2$ powders (Nippon Kagaku) with a 10 nm-thick $LiNbO_3$ coating (Powrex, MP-01) [23,24] and $Li_{10}GeP_2S_{12-x}O_x$ ($x = 0, 0.3, 0.6$) were used as cathodes. The $LiCoO_2$ and $Li_{10}GeP_2S_{12-x}O_x$ powders were weighed in a 70:30 wt ratio and mixed using a vortex mixer for 10 min. Li metal and the $Li_{10}GeP_2S_{12-x}O_x$ pellet were used as the anode and solid electrolyte, respectively. To make the solid electrolyte layer, 100 mg of the $Li_{10}GeP_2S_{12-x}O_x$ powder was pressed into a pellet with a diameter of 10 mm. Lithium foil (thickness, 0.1 mm; diameter, 10 mm) with a Cu mesh current collector and the cathode composite with Al mesh and Al foil current collectors were pressed onto opposite sides of the solid electrolyte pellet. The electrochemical properties of the cells were evaluated using a TOSCAT-3100 (Toyo System). Cycling tests were carried out between 2.5 and 4.2 V for the Li anode at an applied current of 7 mA g^{-1} at 298 K.

3. Results and discussion

3.1. Phase identification of $Li_{10}GeP_2S_{12-x}O_x$ and structural analysis

Fig. 1 shows the XRD patterns of the synthesized samples, which have the general formula $Li_{10}GeP_2S_{12-x}O_x$ ($0 \leq x \leq 1.5$). To confirm the characteristic peaks of the LGPS-type phase and Li_3PO_4 as impurity, magnified patterns around 29.5° and 22.5°, respectively, are also presented. The system can be divided into two composition regions depending on the peak shift, with additional peaks due to Li_3PO_4. For the composition $0 \leq x < 0.9$, a gradual peak shift toward
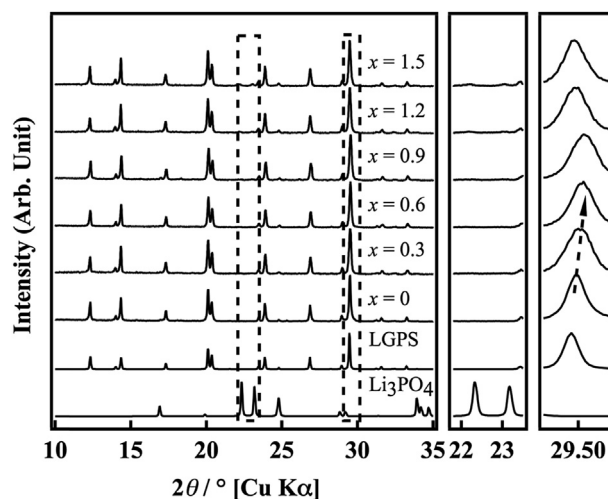

Fig. 1. XRD patterns of $Li_{10}GeP_2S_{12-x}O_x$ ($0 \leq x \leq 1.5$) along with the XRD patterns of Li_3PO_4 (ICSD #79427) and LGPS (ICSD #188887). The magnified patterns around 29.5° and 22.5° are characteristic peaks for LGPS-type phases and Li_3PO_4.